Svorová Pawełkowicz *et al. Herit Sci (2017) 5:27*
DOI 10.1186/s40494-017-0141-6

Heritage Science

RESEARCH ARTICLE

Open Access

Gothic green glazed tile from Malbork Castle: multi-analytical study

Sylwia Svorová Pawełkowicz[1,2,4*], Dana Rohanová[3] and Petr Svora[4]

Abstract

Looking at the *façade* of a historical building, it is often difficult to distinguish between the original decoration and later additions. One such building is the Holy Virgin Mary Church at the Malbork Castle (Northern Poland), built between 1276 and 1406. During the latest restoration works, ceramic tiles with some remnants of the green glaze, decorating the Holy Virgin Mary Church *façade,* were studied in situ using portable X-ray fluorescence spectrometry. Micro-samples were analyzed in laboratory by scanning electron microscopy with energy dispersive X-ray spectrometry (SEM–EDS) and wavelength-dispersive X-ray spectrometry (SEM–WDS), micro-Raman spectroscopy and powder X-ray micro-diffraction. We found that what was originally thought to be a paint layer was in fact a heavily deteriorated SiO_2–PbO glaze. White, yellow and black pigments were found to have been added into the glaze as opacifiers and colorants. Copper and iron were used as glaze colorants. The originally added pigments were transformed into new phases, such as antimony-doped tin oxide. The technology used to produce the glazed tiles was identified. All the results collectively confirmed the medieval origin of the green glazed tiles.

Keywords: Green glazed tile, Silica–lead glaze, Malbork Castle, Medieval technology, Opacifiers, Antimony-doped tin oxide (ATO)

Background

Built by the Order of the Teutonic Knights of St. Mary's Hospital in Jerusalem (*Deutscher Orden*) between about 1276 and 1406 [1], the castle in Malbork (Marienburg) (Fig. 1) is one of the largest medieval monastic fortresses in Europe. The Holy Virgin Mary Church is located in the oldest part of the castle, the so called Upper Castle, erected between 1276 and ca 1300 [1]. Situated on the first floor of the eastern part of the castle's northern wing, it was originally built as a chapel [2]. The peak of the castle's development dates back to 1309, when the headquarters of the Teutonic Order were moved from Venice to Malbork. After 1309 (until 1344) the chapel underwent big construction works—an upper storey was added and the chancel was rebuilt. At that time a huge statue of Virgin Mary with the Child Jesus was placed in a niche on the eastern *façade* of the church.

In the course of the Thirteen Years' War (1454–1466) the Teutonic Order moved to Königsberg and left Malbork Castle to Bohemian mercenaries in payment for their services. In 1457 the citizens of Gdansk bought the castle from them and handed it over to the Polish king Casimir IV Jagiellon. During Polish rule the castle and the church did not change much. In 1626, the church was devastated by Swedish army, while in 1644 a vast fire destroyed the roofs and galleries of the Upper Castle. For a long period the church was used as a storehouse and fell into ruin. As the result of the first Partition of Poland, in 1772 Malbork became part of Kingdom of Prussia. In 1804, pursuant to an edict issued by Frederick William III, king of Prussia, the ruined fortress became a national monument. Because of its political significance, it was possible to find funds for its restoration. Unfortunately, that romantic restoration led to its Neo-Gothicisation. From 1882 until the outbreak of World War II a more respectful restoration took place under the direction of Konrad Steinbrecht, yet nowadays it is sometimes difficult to distinguish between the original decoration and nineteenth century interventions. In 1945, the Holy Virgin Church was largely

*Correspondence: s.pawelkowicz@labko.pl
[1] Biological and Chemical Research Centre, Faculty of Chemistry, University of Warsaw, Żwirki i Wigury 101, 02-089 Warsaw, Poland
Full list of author information is available at the end of the article

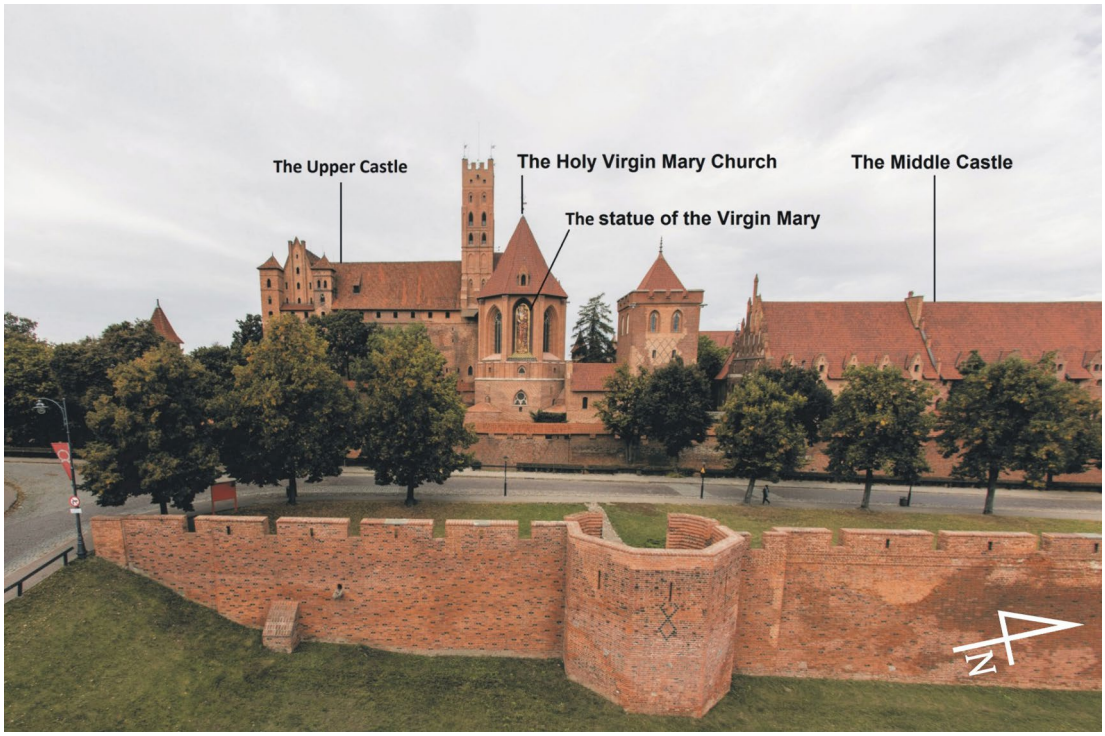

Fig. 1 General view of the Malbork Castle with the statue of the Virgin Mary with the Child Jesus placed on the eastern *façade* of the Holy Virgin Mary Church. Photograph taken after conservation–restoration works in 2016 by D. Kwiecień

damaged, including its roof and vaults, by heavy artillery shelling. In the last 2 years (2014–2016), it underwent extensive conservation and building works [3].

The castle is a representative example of the Red Brick Gothic architectural style with its characteristics ornaments made of dark-glazed headers. The southern *façade* of the church, together with the other three wings of the Upper Castle, forms an inner courtyard decorated with a blind arch frieze with vine ornament made from tiles (Fig. 2a). The oldest tiles, which are studied in the present article, are situated on the eastern part of the southern *façade* of the church (Fig. 2b on the right); they date back to the first construction phase of the castle. They were described in 1989 by Jurkowlaniec [4] as moulded, glazed and fired ceramic tiles and dated to ca 1290. Next to them we see Neo-Gothic replicas (Fig. 2b on the left) introduced in nineteenth century in the place of medieval tiles from the castle's extension after 1309. The Neo-Gothic tiles run along the four *façades* of the inner courtyard of the Upper Castle. The original tiles from the castle's extension are exhibited in the Museum. Interestingly, in a publication from 2010, they are classified as painted [5]. The question has arisen whether the studied tiles were painted or glazed.

Tiles similar to the oldest ones from the first construction phase of the Malbork Castle were found in Elbląg castle (German-*Elbling*) and dated to 1260–1270 [6]. The Malbork Castle tiles are bigger (24 × 24 cm) from the ones from Elbląg (19.5 × 19.5 cm), which clearly shows that different moulds were used for their production. Moreover, no traces of polychromy or glaze were noticed on the Elbląg's tiles. Identical tiles (24 × 24 cm) to the Malbork ones where found in Brandenburg (Polish-*Pokarmin*, Russian-*Ushakovo*) castle and Lochstedt (Russian-*Pavlovo*) castle [6], which means it was a common ornament. As for the tiles from the *façades* of Malbork Castle, findings from 1996 indicate that they could have been used as well for the interior decoration [6].

The chemical composition of glazed building ceramics is widely discussed in the context of tiles from ancient Near East [7, 8] or *azulejos,* typical for Portugal and Spain [9]. Italian medieval glazed brick technology was

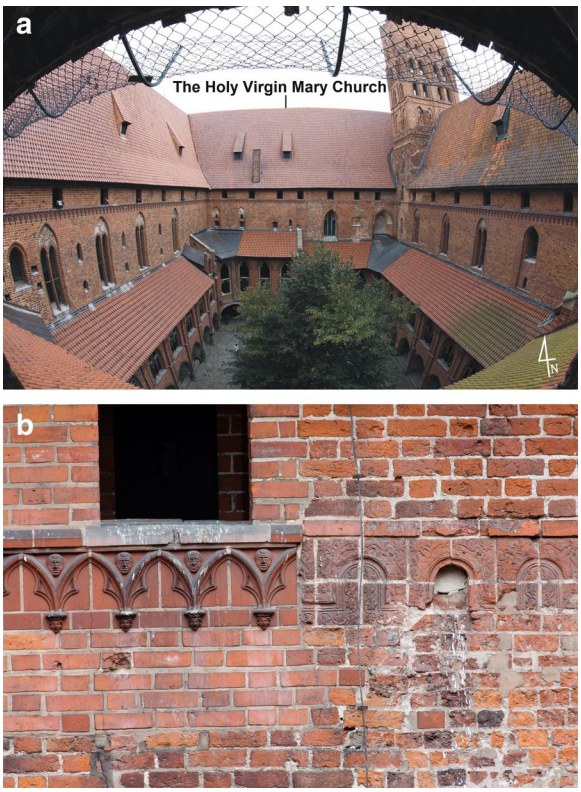

Fig. 2 **a** The blind arch frieze with a vine ornament runs along the four *façades* of the inner courtyard of the Upper Castle. Photograph by D. Kwiecień. **b** Gothic (R) and Neo-Gothic (L) elements on the southern *façade* of the Holy Virgin Church. Photograph by D. Kwiecień

discussed in a recent publication from 2013 [10]. German glazed brick tradition is analyzed with regard to conservation issues [11]. Most studies of glaze concern pottery and archeological findings [12]. On the other hand, medieval architectural ceramics, especially Northern and Central European, still needs to be studied.

The aim of this study, accompanying the recent restoration works conducted in the Upper Castle in Malbork, was to examine and date the green and grey patches of color found on the blind arch frieze with the vine ornament on the *façades* of the Holy Virgin Mary Church (Figs. 2a, b, 3). Our paper presents the results of the analysis of what the restorers initially thought to be a paint layer but in the course of the scientific investigations turned out to be a heavily deteriorated green glaze.

Methods/experimental

Portable X-ray fluorescence (p-XRF)

With the help of art restorers, nine locations were selected, where non-invasive XRF in situ analysis was carried out using a DELTA Premium (Olympus Innov-X, USA) handheld energy dispersive X-ray fluorescence spectrometer equipped with an X-ray lamp with a Rh anode and a silicon drifted detector (SDD). The device enables measurement of elements heavier than Mg ($Z > 12$).

Sample preparation

After p-XRF measurements, and based on the preliminary results, three micro-samples were taken. The samples for stratigraphic studies were embedded in epoxy resin, Epofix (Struers), and polished on a mechanical grinder-polisher Labo-Pol 2 (Struers) using silicon carbide waterproof abrasive foils at successive grits of 180, 320, 500, 1000, 2000, 4000. For the final diamond polishing suspensions of 3 and 1 µm were used. In this paper we present the results obtained mainly for sample II.1.2.1.6. A sampling site is shown in Fig. 3.

Fig. 3 *Green* and *grey* patches of *color* on the ceramic tiles and *grey* patches on mortar joints. Sampling sites. Photograph by D. Kwiecień

Optical microscopy (OM)

Cross-sections of micro-samples were studied (Fig. 4a) both in visible and polarized reflected light using two microscopes: a Leica DM4000 m equipped with a Leica DFC295 camera and an Olympus BX51 equipped with an Olympus E600 camera (Quick Photo Camera 2.3 software).

Electron microscopy (SEM/EDS/WDS)

Cross-sections were inspected (Fig. 4b) with a Jeol scanning electron microscope (SEM) JSM-6510LV equipped with an energy dispersive spectrometer (EDS) by Oxford Instruments with a silicon drifted detector and with a wavelength dispersive X-ray spectrometer (WDS) by Oxford Instruments. Features of EDS: resolution 125 eV (Mn), detection limit 0.1 wt%; features of WDS: resolution 2–10 eV, detection limit 0.01 wt%. EDS measurements were carried out in low vacuum mode under a pressure of 50 Pa and accelerating voltage of 20–25 kV, working distance —10 mm, acquisition time—from 35 to 100 s. For the EDS semi-quantitative results no standardization has been performed. Because of the low content of P, Sn, Sb, Zn (close to or below the EDS detection limit) and possible overlaps between characteristic X-ray peaks of Pb, Mg and As: Pb L_α–As K_α (difference of 8 eV), As L_α–Mg K_α (difference of 28 eV), we took the decision to use the WDS detector. The problematic elements with their X-ray energies are listed in Table 1. For WDS measurements of Mg, P, Zn, As, Sn and Sb the conditions were as follows: high vacuum, accelerating voltage of 25 kV, working distance—10 mm. In order to avoid charging, the sample analyzed with WDS was coated with carbon. Quantitative analyses with EDS were executed after quant optimization on Co standard. Quantitative analyses with WDS were performed after prior standardization. We used as standards Mg, InP, Zn, GaAs, Sn and Sb placed in stainless steel mount produced by SPI. For the standardization of Mg an P their Kα-lines were chosen and for the rest of elements (Zn, As, Sn and Sb) Lα-lines were chosen. The EDS and WDS spectra were analyzed with INCA software by Oxford Instruments. For a glassy matrix and the black particles we present the raw data without normalization to 100%; the results are expressed as oxides wt%.

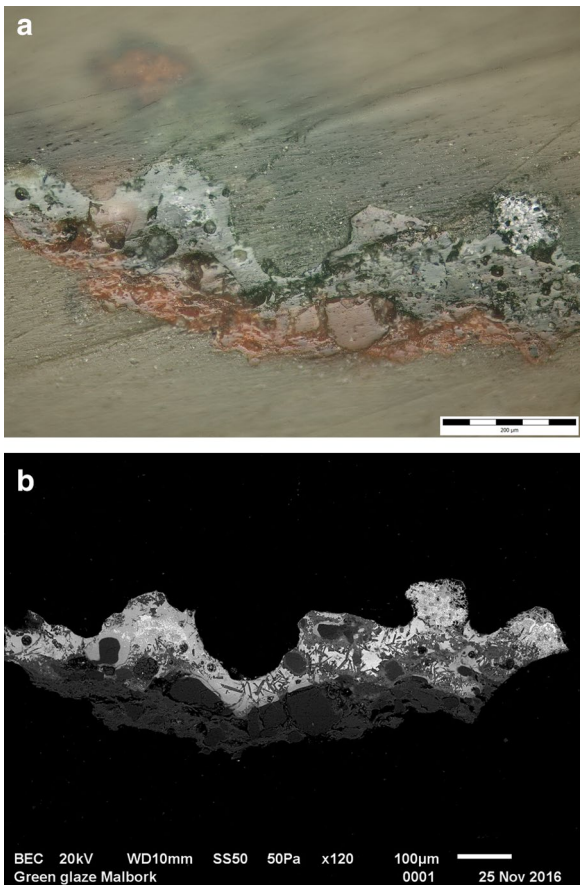

Fig. 4 **a**, **b** Perpendicular cross-section of the green glazed tile from the Holy Virgin Mary Church at Malbork Castle [**a** optical microscopy (OM), **b** backscattered electron composition (SEM/BEC) image]. *Top* glaze (green with white and black particles), *bottom* tile body (*red*)

Table 1 X-ray energies of Mg, P, Zn, As, Sn, Sb and Pb

Element	K_α [eV]	L_α [eV]	M_α [eV]
Mg	1.254	–	–
P	2.010	–	–
Zn	8.637	1.012	–
As	10.543	1.282	–
Sn	25.271	3.444	–
Sb	26.359	3.938	–
Pb	74.969	10.551	2.342

Powder X-ray micro-diffraction (µ-XRD)

Powder X-ray micro-diffraction data were collected from the cross-section with a PANalytical X'Pert PRO diffractometer equipped with a conventional X-ray tube (CoKα radiation with a wavelength of 1.7890 Å, 40 kV, 30 mA, point focus), a glass collimating mono-capillary with an exit diameter of 0.1 mm and a multichannel position sensitive detector (X'Celerator) with an anti-scatter shield. Diffraction patterns were recorded from 4° to 80° in the 2θ interval, counting time of 2200 s per step, step size of 0.0334°. The scan was collected for around 11 h. Qualitative-phase analysis was performed with the HighScore-Plus software package (PANalytical, version 4.5.0) and JCPDS-ICDD PDF-4 database [13].

Micro-Raman spectroscopy

Raman measurements (Figs. 7, 12, 13) were performed with a Nicolet Almega Dispersive Raman Spectrometer, equipped with an Olympus confocal microscope and motorized stage. Depending on the sample properties, 780 or 532 nm excitation line was used. The power of the laser was reduced to 25–50% in order to avoid sample overheating. The typical exposure time was 15–45 s. Each spectrum was collected from two scans. The spectral resolution was about 2 cm^{-1}.

Additional Raman measurements (Figs. 6 and 9) were performed with a Renishaw inVia Reflex micro-Raman spectrometer, equipped with a Leica microscope and motorized stage. The argon 488 nm excitation line was used. The power of the laser was reduced to 10% in order to avoid sample overheating. The spectral resolution was about 2 cm^{-1}.

Results and discussion

In situ measurements

Portable X-ray fluorescence spectrometry

Some green, greyish green and grey patches of color were found on the surface of the tiles, as well as gray patches on mortar joints; they were analyzed with a portable X-ray fluorescence spectrometer (see Table 2). In situ measurements revealed the presence of considerable amount of silicon, sulfur and calcium, and small content of aluminum, potassium, iron, copper and lead. Additionally, tin, antimony and arsenic were detected in green and greyish green areas. In grey areas no copper, tin nor antimony were observed, but some traces of zinc. Strontium, titanium, manganese appeared in minute quantities regardless of the analyzed color [14]. On the basis of preliminary results obtained by p-XRF and macro photographs of the sampling sites (Fig. 3), we interpreted the grey patches as points of dirt accumulation on the top of possible retouches (presence of Zn). The presence of Pb in the grey areas is questionable and most probably overestimated because of spectral interferences and the overlapping peaks of S ($K\alpha_1$ 2.309, $K\beta_1$ 2.465) with Pb lines ($M\alpha_1$ 2.342, $M\beta_1$ 2.444). For further analysis samples from dark green, green and greyish green areas were collected.

Table 2 Estimation of chemical composition in analyzed points (wt%) by p-XRF [14]

Sample	Color	Al	Si	P	S	K	Ca	Ti	Mn	Fe	Cu	Zn	As	Sr	Sn	Sb	Pb
II.1.2.1.7	Green on tile	+++	+++++	+++	+++	+++	+++	++	-	+++	++	-	-	+	-	-	+
II.1.2.1.5	Green on tile	+++	+++++	+++	+++	+++	+++	++	+	+++	+++	-	-	+	++	+	+++
II.1.2.1.6	Dark green on tile	+++	++++	-	++++	++	++++	-	-	+++	+++	-	-	+	++	+	+++
II.1.2.1.4	Greyish green on tile	+++	++++	-	++++	+++	+++	++	+	+++	++	+	-	+	+	+	++
II.1.2.1.3	Grey on tile	+++	++++	-	++++	++	++++	++	-	+++	-	+	-	+	-	-	+
II.1.2.1.2	Grey on mortar joint	-	++++	-	++++	++	++++	-	+	++	-	+	-	+	-	-	+
II.1.2.1.1	Grey on masonry joint	-	++++	-	++++	++	++++	+	+	++	-	+	-	+	-	-	+
II.1.2.1.8	Green on tile	-	++++	-	++++	++	++++	++	-	+++	+++	-	+	+	++	+	++

Legend:

Estimation of the content in wt% in relative scale	+++++	++++	+++	++	+
	50-20	20-5	5-1	1-0.1	<0.1

Analysis of micro-samples

The ceramic body of the green tile

The chemical composition of the crystalline phases of the tile's ceramic body was determined by SEM/EDS (see Table 3—EDS analysis and Fig. 4a, b), μ-XRD (Fig. 5) and micro-Raman spectroscopy (Fig. 6). According to experimental studies, the temperature and the conditions (oxidising or reducing) in the kiln could be deduced from the brick final phase composition [15, 16]. The presence of quartz (SiO_2) and microcline ($K_2O{\cdot}Al_2O_3{\cdot}6SiO_2$) together with the absence of mullite [$Al_{4+2x}Si_{2-2x}O_{10-x}$ (x~0.4)] in the ceramic body indicates that the maximum firing temperature of the Malbork tiles was around 1000 °C [17]. Above 1000 °C microcline disappears completely, while mullite starts to form at around 900 °C [15]. At ca 800 °C calcite and dolomite decomposes [15] and new phases, such as diopside ($CaO{\cdot}MgO{\cdot}2SiO_2$), occur [15, 16]. The presence of diopside ($CaO{\cdot}MgO{\cdot}2SiO_2$) indicates the raw clay material contained calcium and magnesium. In the case of the tiles studied, the higher content of Mg than Ca indicates that dolomite ($CaMg(CO_3)_2$) [18] or simply magnesian calcite (Ca, Mg)CO_3 was present in the raw material rather than calcium carbonate ($CaCO_3$) (Table 3). On the basis of EDS analysis, we can classify the raw material as a Ca-poor clay. The red color of the brick is due to iron oxide—hematite (Fe_2O_3) (confirmed by micro-Raman—Fig. 6). Based on the diffraction pattern obtained from the ceramic body, we can presume some magnetite (Fe_3O_4) might be present as well, although that should be confirmed by other techniques (the lines are at the level of noise) (Fig. 5).

Table 3 The chemical composition of the ceramic body by SEM/EDS [expressed as oxides wt%, normalized to 100%] (an average of the three measurements—an area analysis)

Compound	Na_2O	MgO	Al_2O_3	SiO_2	P_2O_5	K_2O	CaO	TiO_2	FeO	PbO
Feldspar	1.0	nd	16.3	64.4	0.3	13.5	nd	nd	0.4	1.9
Ceramic body mass	2.1	2.1	18.6	55.3	nd	5.6	1.5	0.8	5.7	nd
Quartz	nd	nd	1.0	99.6	nd	nd	nd	nd	nd	nd

nd not determined

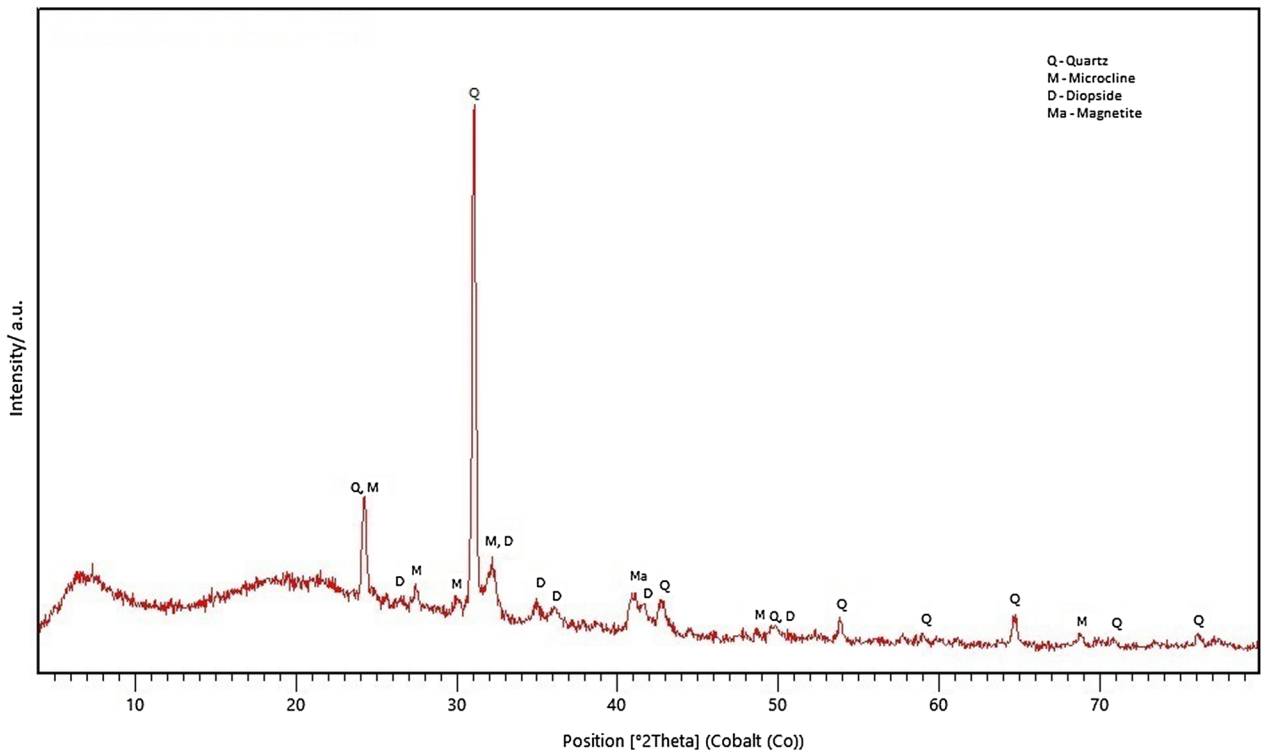

Fig. 5 Diffraction pattern from the ceramic body showing the crystalline phases: quartz (Q), microcline (M), diopside (D) and magnetite (Ma). Author: P. Bezdička

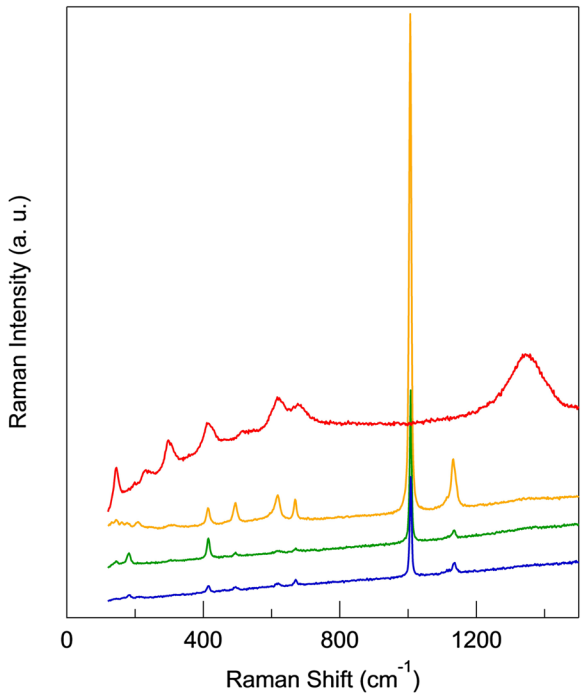

Fig. 6 Raman spectra collected from different *red areas* show the presence of hematite (*red line*) (bands at: ~228, 297, 414, 617, 685, 1340 cm^{-1}) and gypsum (*yellow*, *green* and *blue lines*) (bands at: 414, 493, 617, 669, 1006, 1132 cm^{-1}) in the ceramic body. Author: J. Pokorný

Green glaze

Chemical composition of the green glaze

The chemical analyses of the glassy phase were performed mainly with SEM/EDS; WDS was used for a precise confirmation of the minor elements revealed by in situ XRF analysis but not detected, or on the level of detection limit, in EDS measurements (As, Mg, P, Sn, Sb and Zn) (see "Methods" and Tables 1, 4). We measured the area of pure glass far from the undissolved or recrystallized phases of opacifiers and colorants. The green glaze can be characterized as silica–lead glaze with a low content of alkalis (Na, K, Ca and Mg ≈ 7.7 wt%). Silica–lead–alkali glaze was produced in Near East since 1500 BC [7]. In the West, lead glazes occurred during the Roman era (first century BC—first century AD) [7, 12]. The methods of preparation of silica–lead glazes (high lead and alkali glazes) were described by Tite et al. [19]. Lead in the form of oxide was mixed with silica—in case of high lead glaze, as ground quartz or quartz sand, while in case of alkali glass, quartz was beforehand pre-fritted with alkali [19]. In the case of the Malbork tiles, the results indicate lead was mixed with the mixed-alkali glass (Na, K, Ca, Mg, P confirmed by SEM/EDS/WDS). Phosphorus (confirmed by SEM/WDS) usually comes into the mixed-alkali glass from plant ash [20]. Such glaze mixture was applied on the clay body in water suspension and sometimes mixed with a binder (gum, starch, clay). In our case, tin opacifier and colorants (Cu, Fe, Sb) were added to the mixture and they partly (Sn, Sb, Cu) or completely (Fe) dissolved in the vitreous matrix during firing.

Low concentrations of Sb (0.53%) and Sn (0.51%) were confirmed in the glassy phase by WDS (see Table 4). Results of our previous works [21] show that the concentration of SnO_2 may vary from 0 up to 20 wt% in white opaque glass, depending on the thermal treatment of the sample, solubility of intermediate phases such as $PbSnO_3$ in the glass [22, 23] and place of measurement (SEM/EDS). Low quantities of aluminum detected by EDS (3%) in the glassy matrix are most probably related to the diffusion of elements from the clay body to the glaze during firing as reported by Tite et al. [19], although one may not exclude that some clay [19] was added to the glass frit as well.

The silica–lead glaze applied on the tiles in Malbork as far as the Si/Pb ratio is concerned is similar to Islamic glazes from Zaragoza from eleventh century [24] or to Spanish luster pottery [25], or to some examples of the Italian renaissance maiolica [26].

Opacifiers and colorants

Opacifiers make glass non-transparent and give it a color hue. The oldest known opacifiers were antimony-based: lead antimony yellow and calcium antimonate [23]. Tin-based opacifiers (lead stannate yellow and tin oxide) appeared in Europe for a short time in 2nd–first centuries BC, and then reappeared in the fourth century AD and replaced the antimony-based opacifiers [23]. In the Malbork tiles, we identified a tin-based opacifier—cassiterite SnO_2 (micro-Raman spectroscopy—Fig. 7, and SEM/EDS mapping—Fig. 8), as well as an antimony-based opacifier—Naples yellow (micro-Raman spectroscopy—Fig. 9), which was used rather as colorant (see below). In Venetian's manuscripts cassiterite mixed with silica–lead glass was known as *lattimo* [28]. According to Molera et al. [22], the silica–lead–tin glaze was made in two steps. In the first stage lead and tin, in the form of oxides (PbO, SnO_2), were mixed together and roasted. In the second stage, the powdered metal oxides were mixed with quartz (or alkali glass frit) and then melted and crushed. In this way SnO_2 was evenly distributed in the glass layer, and the glaze was homogenously opacified.

In case of the Malbork tiles, further analyses indicated the use of two yellow pigments—Naples yellow (SEM/EDS, micro-Raman spectroscopy—Fig. 9) and lead–tin yellow type I (SEM/EDS, μ-XRD—Fig. 10), which were probably added as a mixture [29]. According to recipes,

Table 4 Average chemical composition of the green glaze by SEM/EDS/WDS [expressed as oxides wt%]

Compound	Na_2O	MgO	Al_2O_3	SiO_2	P_2O_5	K_2O	CaO	TiO_2	FeO	CuO	PbO	As_2O_3	SnO_2	Sb_2O_3	ZnO
Average	2.1	1.02	3.0	38.3	0.20	1.8	2.8	0.5	3.3	9.4	37.3	0.21	0.51	0.53	0.04
Stdv.	0.6	0.40	0.9	5.0	0.06	0.8	1.4	0.1	0.8	1.9	5.0	0.20	0.19	0.13	0.02
Method	EDS	WDS	EDS	EDS	WDS	EDS	EDS	EDS	EDS	EDS	EDS	WDS	WDS	WDS	WDS

WDS measurements for As, Mg, P, Sn, Sb and Zn

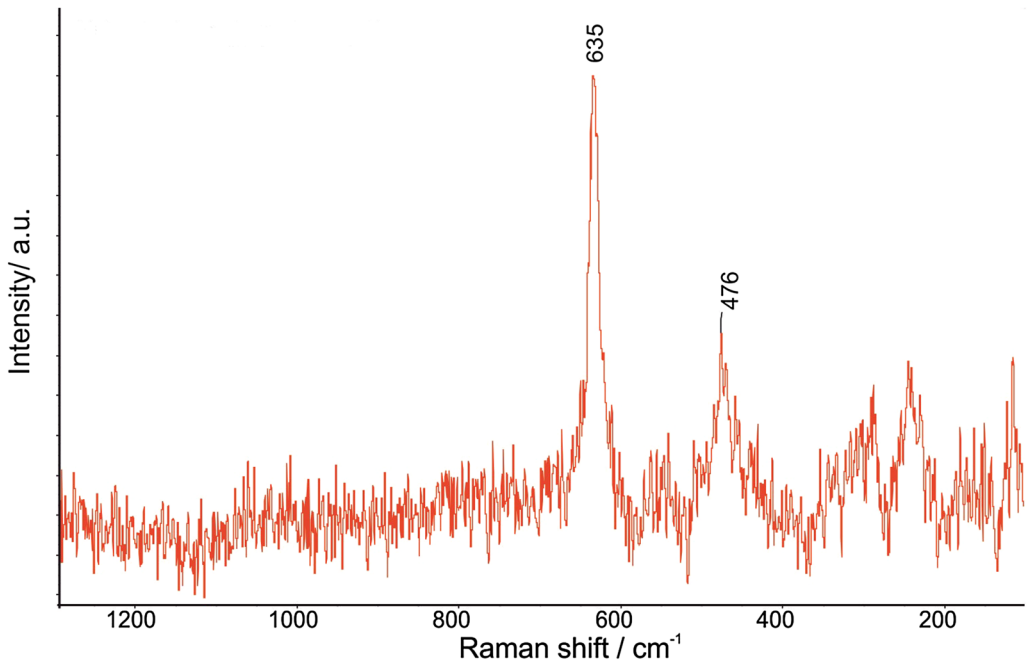

Fig. 7 Raman spectrum of the white pigment—cassiterite (SnO_2). Bands at 635 and 476 cm^{-1}. Author: G. Żukowska

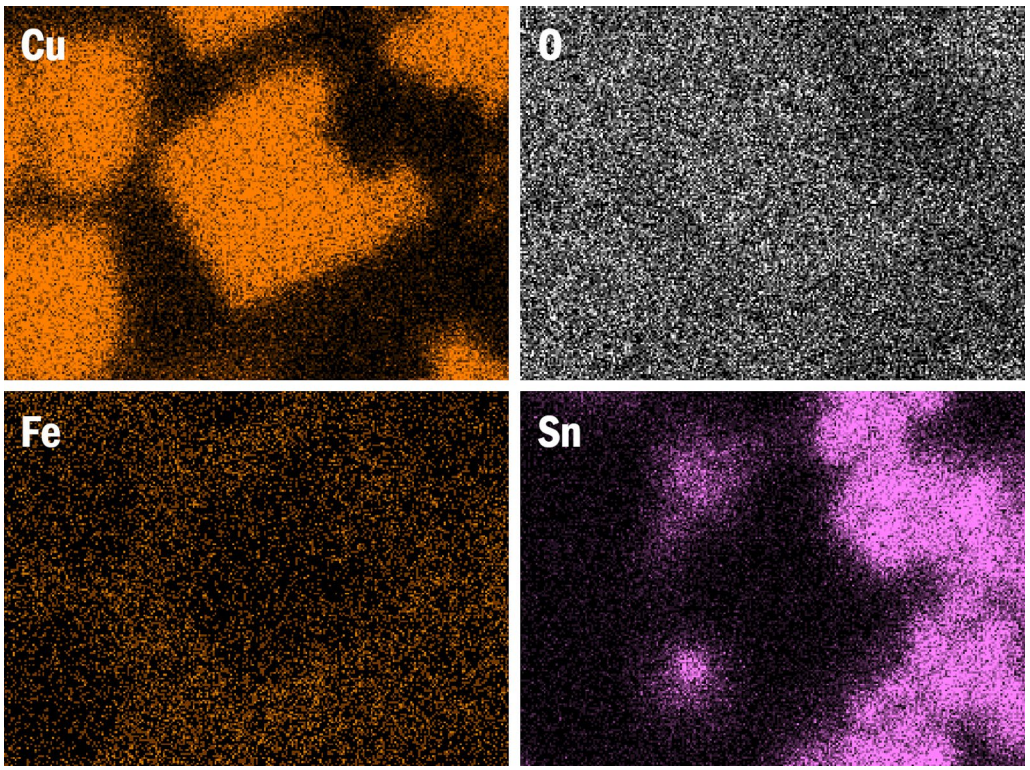

Fig. 8 Cassiterite (Sn) with tenorite (Cu) in the glaze colored with Cu and Fe ions (SEM/EDS mapping)

these two yellow pigments were used in the mixture known as *giallolino* which originated from Germany (*Alemagna*). It appears in manuscripts from the 2nd half of the 15th century, but it is estimated that *giallolino* was applied already about 150 years earlier [28].

Black particles containing Cu were studied by SEM/EDS/WDS (Table 5; Figs. 8, 11) and identified by micro-Raman spectroscopy (Fig. 12) as tenorite (CuO). Undissolved particles of tenorite gave the glaze a darker hue, and that is why some of the rests of glaze found on the vine ornament appeared dark green to almost black. As an initial phase burnt copper (in the form of a mixture of Cu oxides [30]) (e.g. Spanish copper oxide-calcinated metallic Cu) [28] was most probably added. However, we may not exclude that copper filings [30, 31] were added and during the firing process in oxidising atmosphere turned into tenorite. Burnt Cu was widely used in ancient and medieval glasses and glazes [29]. There is also a Renaissance recipe of Piccolpasso (*The Three Books of the Potter's Art*, para. 65–66, 81) described by Tite [32] for a "mixed green", consisting of copper oxide (called "Ramina") mixed with lead oxide and antimony oxide. Tite reports the presence of copper with lead antimonate in the green glazes of Andrea della Robia's panel "Virigin and Child" [32]. According to the author, in that case lead antimonate particles are responsible for the opacification.

The green silica–lead glaze contains relatively high concentrations of dissolved Cu (9.4%) and Fe (3.3%) (expressed as oxides wt%) (Table 4; Fig. 8). The presence of copper in the silica–lead glass gives it a bright green color [33] and in the lead–alkali glazes a bluish green hue [32]. The copper ions present in the glassy matrix are responsible for the green color [30, 34]. Iron ions may give a shade ranging from bright yellow to brown [30]. In the Piccolpasso recipe for yellow color (called "Zallo") we find information about the addition of iron oxide in the form of rust (called "Ferraccia") to yellow antimonate [35]. We assume that copper and iron were added deliberately to the SiO_2–PbO glass. However, it cannot be excluded that part of the iron ions were released from the ceramic body during firing.

Further analyses showed that some new phases were created during the firing process as by-products of the reactions between yellow, white and black colorants and opacifiers. The tin oxide reacted most probably with Naples yellow and a new phase, antimony-doped tin oxide ($Sn_{O.5}Sb_{O.5}O_2$), confirmed by μ-XRD (Fig. 10), EDS mapping (Fig. 11) and micro-Raman spectroscopy (Fig. 13) [36], was formed. The diffraction pattern also shows the presence of wollastonite ($CaSiO_3$) (Fig. 10) which recrystallized from melt. Moreover, a new phase—monimolite ($Pb_3(SbO_4)_2$) was detected by μ-XRD (Fig. 10).

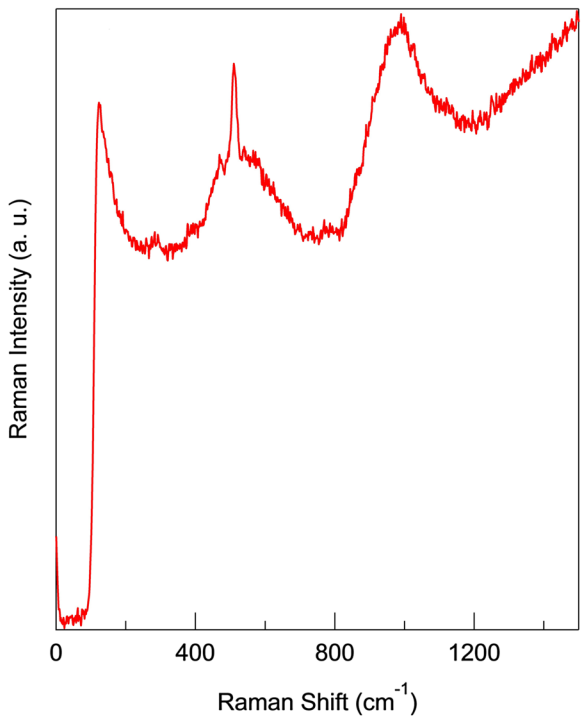

Fig. 9 Raman spectrum of Naples yellow. Bands at: 125, 469, 511 and 950 cm^{-1}. Author: J. Pokorný [27]

Interface

In the glaze layer, we identified unmelted grains of potassium feldspar and quartz (see Fig. 14) (in backscattered electron image, black grains of ca 25–50 μm in diameter). Tite [32] describes a deliberate addition of clay containing potassium feldspar and quartz to glazes applied on maiolica in order to fix better the second layer in the two-layer glaze type. We assume the grains were rather separated from the ceramic body during the application of the wet glaze suspension on the unfired dry body, or later on, during the firing process. Had clay been added deliberately, the particles would be homogenously distributed in the glaze. In SEM/BEC images we observed a noticeable transformation of the potassium feldspar covered by a thin layer of a new phase (containing K–Al–Si and Pb) created during firing (Fig. 14). Plate-shaped crystals at the interface have the same chemical composition as this thin layer (Table 6; Fig. 15). The presence of this phase indicates that the dry ceramic tile was burned together with the glaze in one firing. The interaction of ceramic tile and glaze was described by Tite et al. [19] and Adorni et al. [10]. The authors defined this ceramic body-glaze phase as $K_{0.4}\ Pb_{0.6}\ Al_{1.2}\ Si_{2.7}\ O_7$.

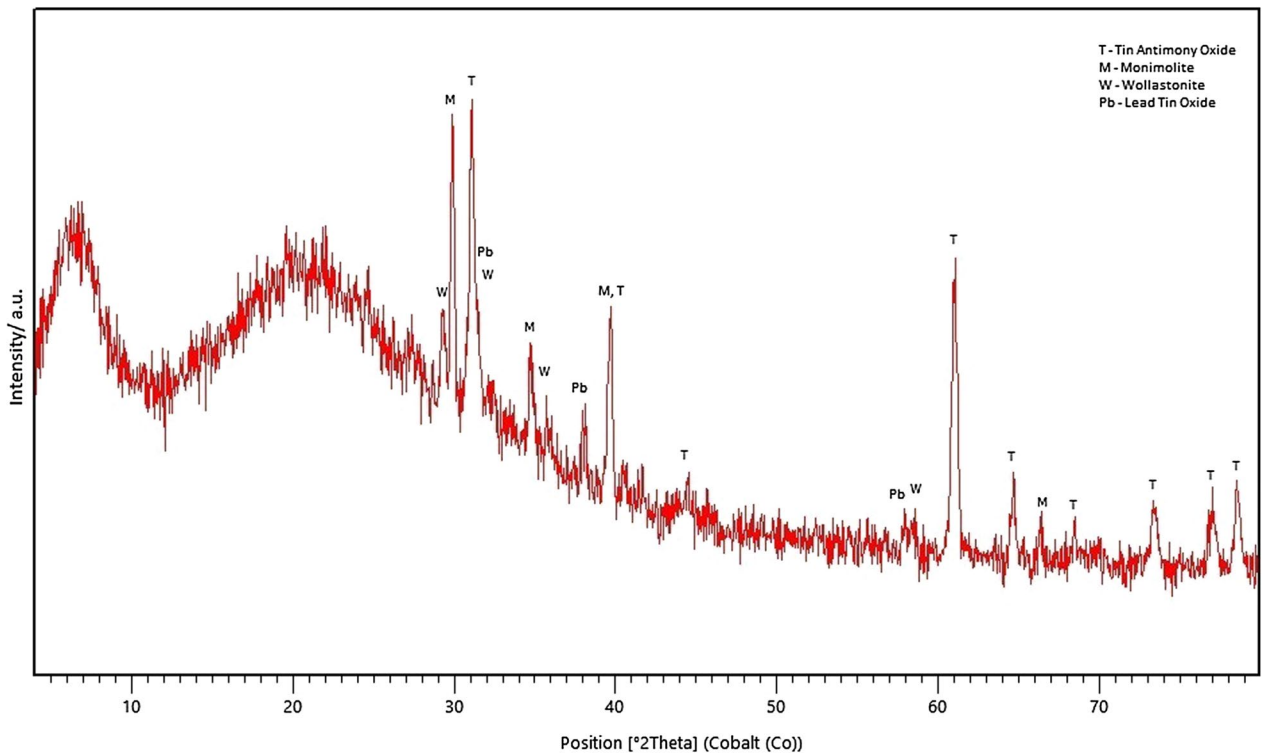

Fig.10 Diffraction pattern from the glaze. *Yellow pigments*: lead tin oxide (Pb_2SnO_4) added to the glaze and newly formed phases during firing—antimony-doped tin oxide ($Sn_{0.5}Sb_{0.5}O_2$), lead antimony oxide—monimolite ($Pb_3(SbO_4)_2$ and wollastonite ($CaSiO_3$). Author: P. Bezdička

Table 5 Average chemical composition of the black particles by SEM/EDS/WDS [expressed as oxides wt%]

Compound	Al_2O_3	SiO_2	SO_3	FeO	CuO	PbO	MgO	P_2O_5	ZnO	SnO_2	Sb_2O_3
Average	0.4	1.7	0.1	0.4	97.2	1.1	0.05	0.07	0.05	0.23	0.46
STDEV.P	0.0	0.7	0.0	0.0	0.6	0.0	0.04	0.00	0.00	0.12	0.42
Method	EDS	EDS	EDS	EDS	EDS	EDS	WDS	WDS	WDS	WDS	WDS

WDS measurements for As, Mg, P, Sn, Sb and Zn

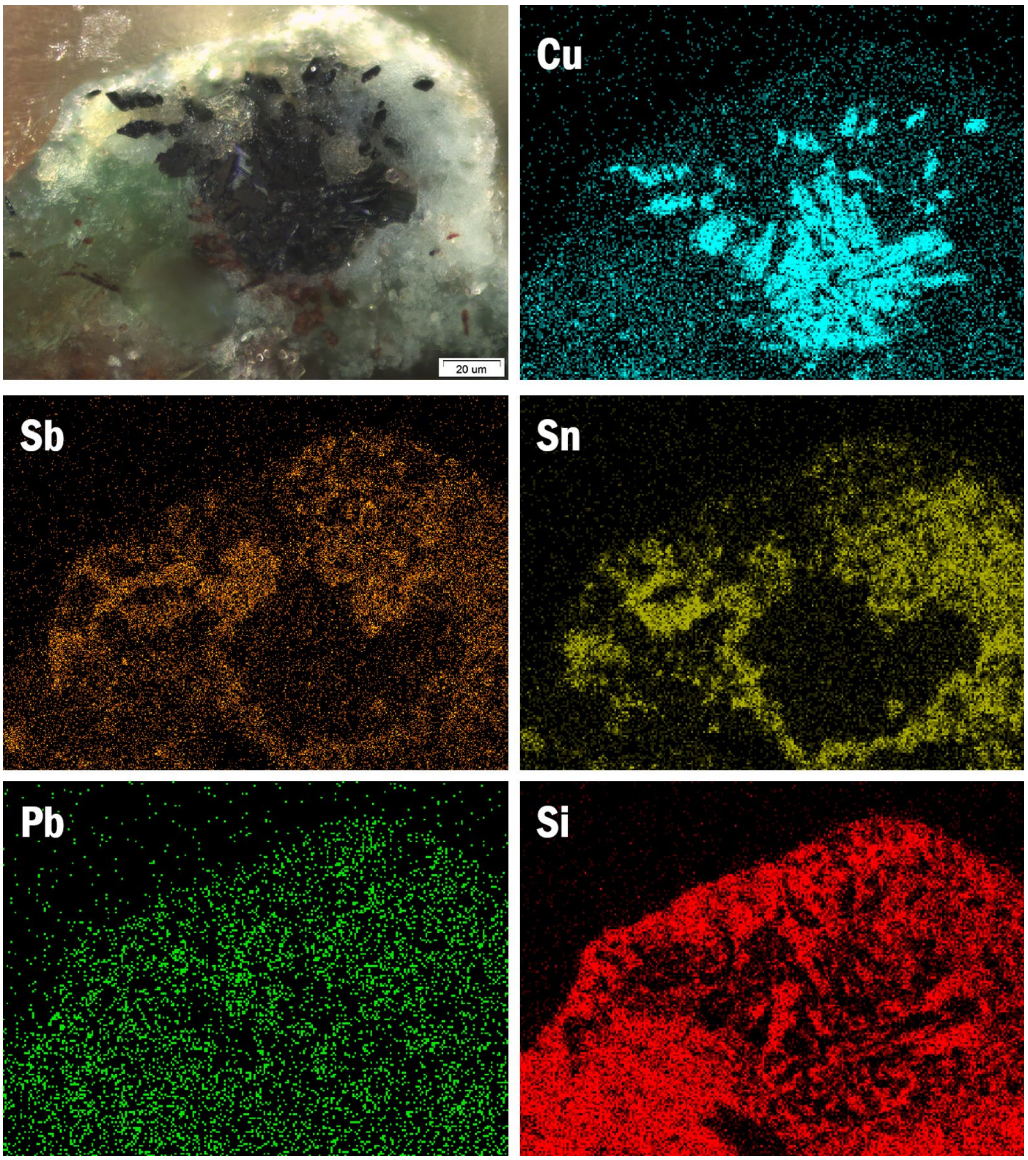

Fig. 11 Black Cu particles surrounded by Sn–Sb phases in a lead–silica glass (SEM/EDS mapping)

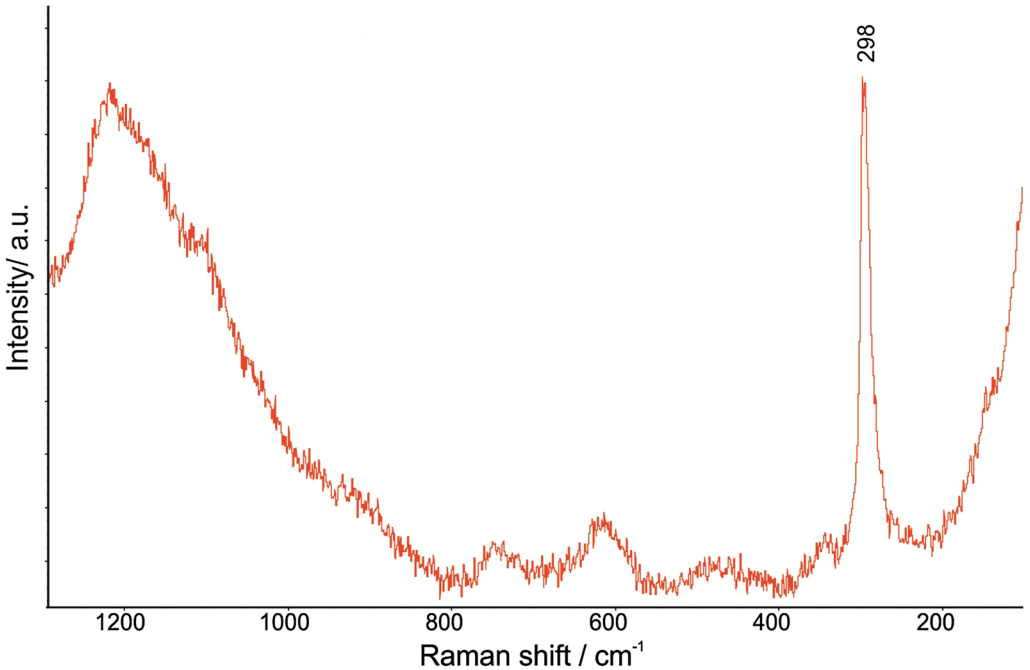

Fig. 12 Raman spectrum of black Cu-bearing mineral–tenorite (CuO). Bands at 298 and 611 cm^{-1} Author: G. Żukowska

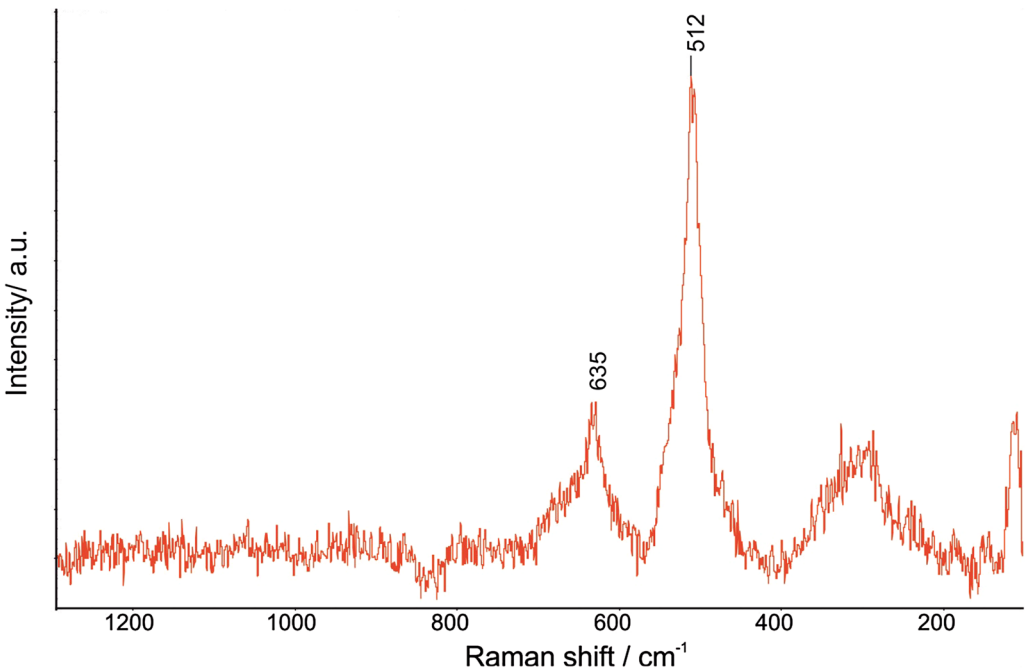

Fig. 13 Raman spectrum of antimony-doped tin oxide. Bands at 635, 512 and around 330 cm^{-1}. Author: G. Żukowska [37]

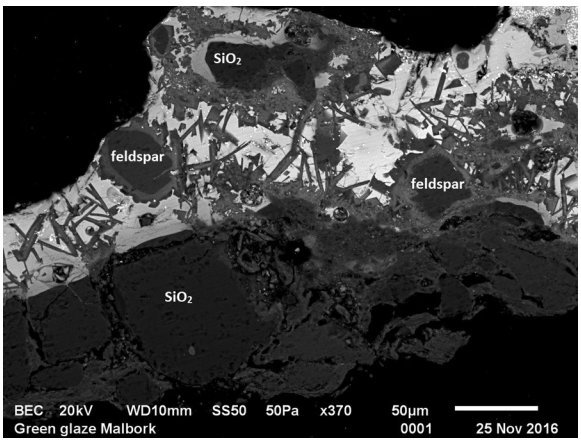

Fig. 14 Detail of the interface "green glaze-tile body". Grains of feldspar (*dark grey*) are covered by a lighter, thin layer (containing K–Al–Si–Pb) (SEM/BEC image)

Glaze devitrification

A secondary crystallized phase, containing Si–Ca–Mg and Fe (Fig. 16), was formed during cooling (devitrification) in the glassy matrix. It is possible that it is a solid solution of diopside ($CaO{\cdot}MgO{\cdot}2SiO_2$) and hedenbergite ($CaO{\cdot}FeO{\cdot}2SiO_2$) (confirmed by SEM/EDS) [12, 37].

The separated feldspar grains, together with unmelted SiO_2, newly formed crystals (K–Al–Si–Pb, diopside and wollastonite) as well as gas bubbles increase the opacity of the glaze.

Ageing (deterioration and corrosion)

The poor state of preservation of the glaze may be linked with harsh weather conditions—big changes in relative humidity and ambient temperature—that led to formation of cracks in the surface layer of the tiles. The climate in Malbork is classified by Koppen as humid continental, which means the tiles are exposed to high humidity. As

Table 6 The chemical composition of the interface by SEM/EDS [expressed as oxides wt%] (an average of the three measurements)

Compound	Na_2O	MgO	Al_2O_3	SiO_2	P_2O_5	K_2O	CaO	TiO_2	FeO	PbO
Interface	nd	nd	14.5	59.8	nd	8.1	1.3	0.3	2.5	9.4

nd not determined

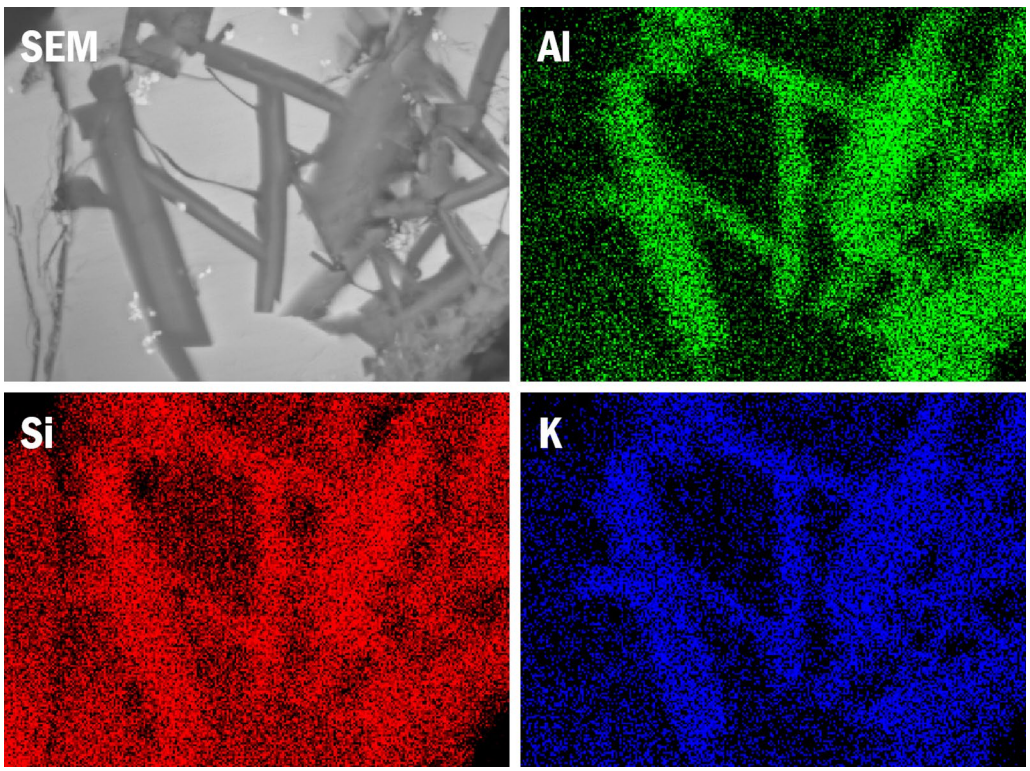

Fig. 15 Interface phase K–Al–Si–Pb (SEM/EDS mapping)

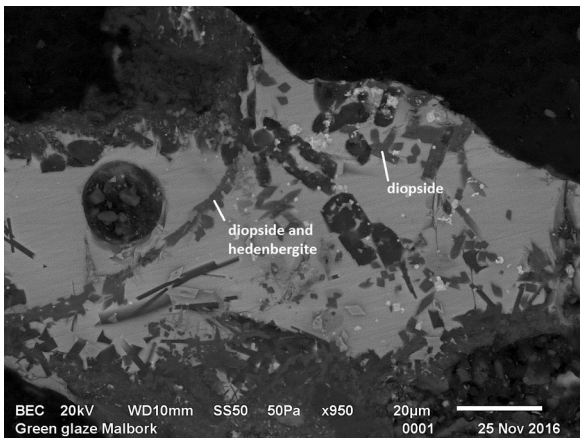

Fig. 16 Tabular crystals of a solid solution (the *lighter grey*) containing SiO_2, CaO, MgO and FeO (SEM/BEC image, *left side*, next to the big bubble)

Malbork is situated in the coastal area (ca 40 km from the Baltic sea), NaCl could penetrate the glaze through the microcracks. Water, when freezing in the microcracks expands in volume and causes fractures. Porous materials, such as ceramics, absorb water during the rain and expand. Moisture expansion of the ceramic body is a known phenomenon [38, 39]. The tiles studied are situated on the southern façade, so they dry quickly, loose water and shrink. Differences in moisture expansion between the body and glaze may possibly have influenced the glaze detachment. Another corrosion product is gypsum, found by micro-Raman spectroscopy in the ceramic body (Fig. 6). The calcium carbonate from the brick or adjacent mortar joints reacted with sulphur in the air and formed gypsum—process known as sulphation or chemical weathering [40].

Conclusion

The glaze studied turned out to be a very complicated system. In order to unveil the secrets of its production we used a set of analytical methods. The morphology of the interface layer together with the composition of the glassy matrix and ceramic body clearly show that the glaze was applied on the dried clay body and fired in the kiln at one step at the temperature less than 1000 °C, but certainly more than 800 °C. The silica–lead glaze applied on the ceramic tile was colored with copper and iron ions and opacified/colored using the artificially prepared pigments—white (cassiterite SnO_2 melted with PbO before adding to the glass), yellow (mixture of Naples yellow and lead tin oxide type I), copper filings (most probably in the form of oxides as burnt copper). The originally added yellow and white pigments were transformed into new phases, such as Sb-doped tin oxide ($Sn_{0.5}Sb_{0.5}O_2$) or monimolite ($Pb_3(SbO_4)_2$). Tin-opacified glazes have a long history. We observed some similarities between Malbork's glaze with Zaragoza glazes from 11th c. (Si/Pb ratio) and also with Italian maiolica (Si/Pb ratio, copper oxide and lead antimonate mixture). The technologies used confirmed the medieval origin of the green glazed tiles.

Abbreviations

p-XRF: portable X-ray fluorescence spectrometry; SEM: scanning electron microscopy; BEC: backscattered electron composition image; EDS: energy dispersive X-ray spectrometry; WDS: wavelength-dispersive X-ray spectrometry; µ-XRD: powder X-ray micro-diffraction.

Authors' contributions

SSP coordinated the overall project, collected the samples, prepared the cross-sections, performed some of the EDS measurements, interpreted the Raman spectra and wrote the paper together with DR. PS performed the EDS and WDS measurements, interpreted the diffraction patterns and wrote about electron microscopy. DR planned further EDS analysis, interpreted the data obtained taking into account the knowledge in the field of glass technology and wrote the paper together with SSP. All authors read and approved the final manuscript.

Author details

[1] Biological and Chemical Research Centre, Faculty of Chemistry, University of Warsaw, Żwirki i Wigury 101, 02-089 Warsaw, Poland. [2] Faculty of Conservation and Restoration of Works of Art, Academy of Fine Arts in Warsaw, Wybrzeże Kościuszkowskie 37, 00-379 Warsaw, Poland. [3] Department of Glass and Ceramics, University of Chemistry and Technology, Technická 5, 166 28 Prague 6, Czech Republic. [4] Institute of Inorganic Chemistry, The Czech Academy of Sciences, Husinec-Řež 1001, 250 68 Řež, Czech Republic.

Acknowledgements

The authors would like to thank the consortium Monument Service, Gorek Restauro, POiKZ Malbork for providing the samples and co-funding the research. SSP would like to thank professor Maria Poksińska from Nicolaus Copernicus University in Toruń for her precious advice. A special thanks to Dr. David Hradil, RNDr. Janka Hradilová (ALMA Laboratory, Prague) for p-XRF measurements, Dr. RNDr Petr Bezdička (ALMA Laboratory, Prague) for µ-XRD measurements and help in data interpretation, dr Grażyna Żukowska (Chemical Faculty, Warsaw University of Technology) and Jan Pokorný (Institute of Physics of the Czech Academy of Sciences) for micro-Raman spectroscopy measurements. We also wish to extend our thanks to Ing. Alexandra Kloužková, CSc. (Department of Glass and Ceramics, University of Chemistry and Technology Prague) for valuable advice. We extend special gratitude to Grzegorz Muszyński for linguistic improvements.

Competing interests

The authors declare that they have no competing interests.

Funding

The research was carried out within the framework of the project "Conservation and building works in the complex of the Holy Virgin Church in the Castle Museum in Malbork", co-funded from the European Economic Area Financial Mechanism for the years 2009–2014 (EEA FM 2009–2014), within the Programme Conservation and revitalisation of cultural heritage.

Writing the manuscript was possible thanks to the funding of Academy of Fine Arts in Warsaw, Faculty of Conservation and Restoration of Works of Arts. The research project was supported by the National Science Centre in Poland (Grant No. UMO-2015/19/N/HS2/03503). Principal Investigator: Sylwia Svorová Pawełkowicz.

Publisher's Note

Received: 7 October 2016 Accepted: 12 May 2017
Published online: 12 July 2017

References

1. Emery A. Malbork castle–Poland. Castle Stud Group J. 2007;21:138–156. http://www.castlestudiesgroup.org.uk/Malbork%20-%20Anthony%20Emery.pdf. Accessed 3 Sept 2016.
2. Kittel K. Kościół NMP–zagadnienia historyczne, unpublished report; 2016.
3. http://www.funduszeeog.zamek.malbork.pl/index.php?mod=aktualnosci&aid=20. Accessed 11 Dec 2016.
4. Jurkowlaniec T. Gotycka rzeźba architektoniczna w Prusach. Wrocław: Ossolineum; 1989.
5. Jesionowski B. Segmenty fryzu arkadkowego, ok. 1300–1310. In: Pospieszna B, editor. Fundacje artystyczne na terenie państwa krzyżackiego w Prusach. Katalog wystawy w Muzeum Zamkowym w Malborku. Malbork: Muzeum Zamkowe; 2010.
6. Rynkiewicz-Domino W. Trzy płytki fryzu ornamentalnego, ok. 1260–1270. In: Pospieszna B, editor. Fundacje artystyczne na terenie państwa krzyżackiego w Prusach. Katalog wystawy w Muzeum Zamkowym w Malborku. Malbork: Muzeum Zamkowe; 2010.
7. Moorey PRS. Ancient Mesopotamian materials and industries. Oxford: Oxford University Press; 1994.
8. Aloiz E, Douglas JG, Nagel A. Painted plaster and glazed brick fragments from achaemenid pasargadae and persepolis, Iran. Herit Sci. 2016;4:3. doi:10.1186/s40494-016-0072-7.
9. Coentro S, Mimoso JM, Lima AM, Silva AS, Pais AN, Muralha VSF. Multi-analytical identification of pigments and pigment mixtures used in 17th century Portuguese *azulejos*. J Eur Ceram Soc. 2012;32:37–48. doi:10.1016/j.jeurceramsoc.2011.07.021.
10. Adorni E. The steeple spire of the Parma Cathedral. An analysis of the glazed bricks and mortars. J Eur Ceram Soc. 2013;33(13):2801–9. doi:10.1016/j.jeurceramsoc.2013.04.019.
11. Schwarz HJ, Stadlbauer E. Conservation and restoration methods of glazed architectural ceramics. Conserv Restor Bull. 2005;16:54–9.
12. Mason RB, Tite MS. The beginnings of Tin-opacification of pottery glazes. Archaeoemtry. 1997;39:41–58. doi:10.1111/j.1475-4754.1997.tb00789.x.
13. International Centre for Diffraction Data, Newtown Square, PA, USA release 54; 2016.
14. Hradil D, Hradilová J. Investigations in Malbork and Kwidzyn: results of non-invasive screening of wall paintings in Malbork. Prague: ALMA laboratory-unpublished report. 2015.
15. Cultrone G, Rodriguez-Navarro C, Sebastian E, Cazalla O, De La Torre MJ. Carbonate and silicate phase reactions during ceramic firing. Eur J Mineral. 2001;13:621–34. doi:10.1127/0935-1221/2001/0013-0621.
16. Lopez-Arce P, Garcia-Guinea J, Gracia M, Obis J. Bricks in historical buildings of Toledo City: characterisation and restoration. Mater Charact. 2003;50:59–68. doi:10.1016/S1044-5803(03)00101-3.
17. Kloužková A, Zemenová P, Kohoutková M, Mazač Z. Ageing of fired-clay ceramics: comparative study of rehydroxylation processes in a kaolinitic raw material and moon-shaped ceramic idol from the bronze age. Appl Clay Sci. 2016;119(2):358–64. doi:10.1016/j.clay.2015.11.002.
18. Hlaváč J. The technology of glass and ceramics, an introduction, Glass science and technology 4. New York: Elsevier Scientific Publishing Company; 1983.
19. Tite MS, Freestone J, Mason R, Molera J, Vendrell-Saz M, Wood N. Review article: lead glazes in antiquity—methods of production and reasons for use. Archaeometry. 1998;40:241–60. doi:10.1111/j.1475-4754.1998.tb00836.x.
20. Tite MS, Shortland A, Maniatis Y, Kavoussanaki D, Harris SA. The composition of the soda-rich and mixed alkali plant ashes used in the production of glass. J Archaeol Sci. 2006;33:1284–92. doi:10.1016/j.jas.2006.01.004.
21. Rohanová D, Sedláčková H. Venetian filigrana glass and its imitations made in central Europe: comparison of a typology and a chemical composition. J Glass Stud. 2015;57:295–309.
22. Molera J, Pradell T, Salvado N, Vendrell-Saz M. Evidence of tin oxide recrystallization in opacified lead glazes. J Am Ceram Soc. 1999;82(10):2871–5. doi:10.1111/j.1151-2916.1999.tb02170.x.
23. Tite M, Pradell T, Shortland A. Discovery, production and use of tin-based opacifiers in glasses, enamels and glazes from the late iron age onwards: a reassessment. Archaeometry. 2008;50(1):67–84. doi:10.1111/j.1475-4754.2007.00339.x.
24. Molera J, Vendrell-Saz M. Chemical and textural characterization of tin glazes in islamic ceramics from eastern spain. J Archaeol Sci. 2001;28:331–40. doi:10.1006/jasc.2000.0606.
25. Peréz-Arantegui J, Molera J, Larrea A, Pradell T, Vendrell-Saz M. Luster pottery from the thirteenth century to the sixteenth century: a nanostructured thin metallic film. J Am Ceram Soc. 2001;84(2):442–6. doi:10.1111/j.1151-2916.2001.tb00674.x.
26. Antonelli F, Ermeti AL, Lazzarini L, Verità M, Raffaelli G. An archaeometric contribution to the characterization of renaissance maiolica from urbino and a comparison with coeval Maiolica from Pesaro (The Marches, Central Italy). Archaeometry. 2014;56(5):784–804. doi:10.1111/arcm.12045.
27. Rosi F, Manuali V, Grygar T, Bezdička P, Brunetti BG, Sgamellotti A, Burgio L, Seccaroni C, Miliani C. Raman scattering features of lead pyroantimonate compounds: implication for the non-invasive identification of yellow pigments on ancient ceramics. Part II. *In situ* characterisation of Renaissance plates by portable micro-Raman and XRF studies. J Raman Spectrosc. 2011;42:407–14. doi:10.1002/jrs.2699.
28. Moretti C, Toninato T, Watts DC. Glass recipes of the renaissance, transcription of an anonymous venetian manuscript. Barnet: Watts Publishing; 2011.
29. Hradil D, Grygar T, Hradilová J, Bezdička P, Grünwaldová V, Fogaš I, Miliani C. Microanalytical identification of Pb-Sb-Sn yellow pigment in historical European paintings and its differentiation from lead tin and Naples yellows. J Cult Herit. 2007;8:377–86. doi:10.1016/j.culher.2007.07.001.
30. Eggert G, Hillebrecht H. The enigma of the emerald green—medieval lead glass vessels à la heraclius. In: Jerem E, Biró KT, editors. Archaeometry 98. Proceedings of the 31st Symposium. Oxford: B.A.R. Int. Ser. 1043 (Vol. II). p. 525–530.
31. Heraclius, De coloribus et artibus Romanorum, Liber III, 3, 7, 8. https://www.hs-augsburg.de/~harsch/Chronologia/Lspost10/Heraclius/her_col3.html. Accessed 6 Mar 2017.
32. Tite MS. The production technology of Italian maiolica: a reassessment. J Archaeol Sci. 2009;36:2065–80. doi:10.1016/j.jas.2009.07.006.
33. Kloužková A, Kohoutková M, Blažková G, Zemenová P, Kavanová M. Material Finds from the Renaissance Waste Pits at Prague Castle, Casum Pragensie, part II. Prague: Archeologický ústav AVCR; 2016. Part II, p. 233.
34. Colomban P. Glasses, glazes and ceramics-recognition of the ancient technology from the Raman spectra. In: Edwards HG, Chalmers JM, editors. Raman spectroscopy in archaeology and art history. Cambridge: Royal Society of Chemistry; 2004. p. 192–206.
35. Carratoni L, Di Santo Albertali VA. Micro-Raman investigation of coloured glazes on majolica sherds from the Monk's Palace waste shaft in Capena (Rome). J Appl Las Spectrosc. 2015;2(1):20–8.
36. Müller V, Rasp M, Štefanić G, Ba J, Günther S, Rathousky J, Niederberger M, Fattakhova-Rohlfing D. Highly conducting nanosized monodisperded antimony-doped tin oxide particles synthesized via nonaqueous sol-gel procedure. Chem Mater. 2009;21:5229–36. doi:10.1021/cm902189r.
37. Bartuška M. Vady skla. Prague: Glass Centrum Valašské Meziříčí; 2001.
38. Kloužková A, Kavanová M, Kohoutková M, Zemenová P, Dragoun Z. Identification of causes of degradation of Gothic ceramic tiles by thermal analyses. J Therm Anal Calorim. 2016;125:1311–8. doi:10.1007/s10973-016-5488-5.
39. Plešingerová B, Klapáč M, Kovalčíková M. Moisture expansion of porous biscuit bodies-reason of glaze cracking. Ceram Silikáty. 2002;46(4):159–65.
40. Lopez-Arce P, Garcia-Guinea J. Weathering traces in ancient bricks from historic buildings. Build Environ. 2005;40(7):929–41. doi:10.1016/j.buildenv.2004.08.027.